MODELLING OF DISPERSOID AND CONSTITUENT PARTICLE EVOLUTION IN 3XXX ALLOYS

J.P. Suni and R.T. Shuey

Alcoa Technical Center, Alcoa Center, PA 15069

ABSTRACT

A kinetic model is described for dispersoid and constituent particle evolution during preheating of 3XXX alloys. Dispersoid modelling combines the parallel processes of nucleation, growth and coarsening, resulting in evolution equations for number density and volume fraction of dispersoid. Constituent modelling combines the parallel processes of growth (or dissolution) and transformation from Al_6[Fe,Mn] to Al_{12}[Fe,Mn]$_3$Si phases, resulting in evolution equations for volume fractions of these phases, as well as Mg_2Si. The evolution equations for dispersoids and constituents are coupled to each other through the matrix concentrations of manganese and silicon. Adjustable parameters relate to nucleation kinetics, interfacial energy and equilibrium solvi. The model is fit to conductivity data, dispersoid size measurements and constituent characterization. The data contain variations in solidification rate, alloy composition and thermal history. The resulting model can be used to predict effects of process excursions, or to search for new combinations of alloy composition and thermal practice, on the basis of physical principles and prior data.

Keywords: Model, dispersoids, constituents, precipitation, nucleation, growth, coarsening.

1. INTRODUCTION

The evolution of dispersoid and constituent particles is an important aspect in the development of microstructure in most commercial aluminum alloys. This is particularly true for 3xxx alloys, where these particles can have a significant impact on processing and formability, with lesser effect on strength. A mathematical model is an attractive way to describe dispersoid and constituent evolution, because the response of these particles to time, temperature and composition can be non-monotonic and is difficult to parameterize simply. A number of researchers have developed modelling approaches to particle evolution. Goodrich[1] used an Avrami type formulation to model dispersoid kinetics for 3004 ingots. Work has been done at SINTEF over the past few years[2,3] to model the as cast state and the evolution of solute content, dispersoids and constituents during preheating of 3xxx alloys. The model developed for the present work is described below.

2. MODEL DETAILS

2.1 Dispersoids

For the purposes of modelling commercial 3003, 3004 and similar alloys, only Al_{12} type dispersoids are considered. This limits application to intermediate Mn/Si ratios. Dispersoid particles are assumed to be spherical, and manganese diffusivity is considered rate limiting. Dispersoids are characterized by two independent quantities, namely volume fraction, f_d and number density, N_v. Evolution consists of nucleation, growth and coarsening. Nucleation consists of introducing new particles and, thus (positively) influences number density and volume fraction. Growth involves adding onto or removing material from particles and, thus influences volume fraction (in either way), but not number density. Dissolution is simply negative growth. Coarsening is the mass transfer from small to large particles, driven by interfacial energy, and it influences (negatively) number density, but not volume fraction. These processes can be

superposed as follows, where the subscripts n,g,c refer to nucleation, growth and coarsening, respectively.

$$\frac{dN_v}{dt} = \left.\frac{dN_v}{dt}\right)_n + \left.\frac{dN_v}{dt}\right)_c \quad (1)$$

$$\frac{df_d}{dt} = \left.\frac{df_d}{dt}\right)_n + \left.\frac{df_d}{dt}\right)_g \quad (2)$$

2.1.1 Nucleation

The nucleation rate is given by:

$$\left.\frac{dN_v}{dt}\right)_n = \frac{4\pi r^{*2} D_{Mn} \cdot (N_{v0} - N_v)}{b^4} \cdot e^{\frac{-4\pi B r^{*2}\sigma}{3kT}} \quad (3)$$

Here, B is less than one and is a dimensionless correction from the classical homogeneous nucleation rate equation, physically representing a reduction in the energy barrier to nucleation. Also in Equation 3, b is the interatomic spacing, k is boltzman's constant, σ is the interfacial energy and N_{v0} is the total number of sites at which nucleation can occur. Further, D_{Mn} is the diffusivity of manganese. The term r* is the critical radius for homogeneous nucleation.[4,5]

The first term on the right hand side of Equation 2 can be written by inspection, assuming nucleation creates spherical particles of radius r*, i.e.

$$\left.\frac{df_d}{dt}\right)_n = \frac{4}{3}\pi r^{*3} \cdot \left.\frac{dN_v}{dt}\right)_n \quad (4)$$

2.1.2 Growth and Coarsening

The following equation for the growth rate of the average particle size, $\bar{r}$ can be derived by slight adjustment of the steady state growth law for an isolated particle:[4]

$$\frac{d\bar{r}}{dt} = \frac{k_g \cdot D_{Mn}}{m\bar{r}} \cdot \left(\frac{[Mn] - [Mn]_{e,m\bar{r}}}{\{Mn\} - [Mn]_{e,m\bar{r}}}\right) \quad (5)$$

Here, the bracketed quantity, [Mn] refers to solute manganese and the braced quantity, {Mn} refers to the density adjusted weight percent of manganese in the precipitate. The subscripted solute manganese term, $[Mn]_{e,m\bar{r}}$ refers to the Gibbs-Thompson adjusted equilibrium solute content at a radius that is a factor "m" times the average radius. The term, k_g is a dimensionless adjustment constant. The term, m is taken to be 1.25, which is a compromise between extremes for pure growth of a log normal distribution[6] and for traditional LSW coarsening.[7] Equation 5 can be separated into two terms, representing pure growth/dissolution and pure coarsening, i.e.

$$\frac{d\bar{r}}{dt} = \frac{k_g \cdot D_{Mn}}{m\bar{r}} \cdot \left(\frac{[Mn] - [Mn]_{e,\bar{r}}}{\{Mn\}' - [Mn]_{e,m\bar{r}}}\right) + \frac{k_g \cdot D_{Mn}}{m\bar{r}} \cdot \left(\frac{[Mn]_{e,\bar{r}} - [Mn]_{e,m\bar{r}}}{\{Mn\}' - [Mn]_{e,m\bar{r}}}\right) \quad (6)$$

or

$$\frac{d\bar{r}}{dt} = \left.\frac{d\bar{r}}{dt}\right)_g + \left.\frac{d\bar{r}}{dt}\right)_c \quad (7)$$

The second term on the right hand side of Equation 1 can be obtained by combining Equations 6 and 7 with the following equation:

$$\left.\frac{dN_v}{dt}\right)_c = -\frac{3N_v}{\bar{r}} \cdot \left.\frac{d\bar{r}}{dt}\right)_c \quad (8)$$

The second term on the right hand side of Equation 2 can be obtained by combining Equations 6 and 7 with the following equation:

$$\left.\frac{df_d}{dt}\right)_g = \frac{3 \cdot f_d}{\bar{r}} \cdot \left.\frac{d\bar{r}}{dt}\right)_g \tag{9}$$

These constitute the evolutionary equations for number density, N_v and volume fraction, f_d. These equations, plus equilibrium equations and diffusivities, allow these two independent dispersoid quantities to be calculated for arbitrary temperature history.

2.2 Constituents

The volume fractions of five independently evolving constituent phases, namely Al_6Fe, Al_6Mn, $Al_{12}Fe_3Si$, $Al_{12}Mn_3Si$ and Mg_2Si, are calculated. These constituent phases are assumed to exist only in the interdendritic regions and are, thus morphologically distinct from the dispersoids treated above. Evolution of these volume fractions, labeled as f_1 to f_5, respectively, is by two processes, namely growth (or dissolution) and transformation of Al_6 to Al_{12} type constituents. Thus, evolution equations for constituent volume fractions can be written generally as follows, where the subscripts x and g refer to transformation and growth, respectively:

$$\frac{df_i}{dt} = \left.\frac{df_i}{dt}\right)_g + \left.\frac{df_i}{dt}\right)_x \tag{10}$$

Growth of iron bearing constituents, f_1 and f_3 is negligible, leaving three volume fractions which can grow or dissolve. The constituent Mg_2Si is not involved in transformation, leaving four volume fractions which can change by transformation. The constituent growth rate term in Equation 10 is obtained by assuming the limiting factor is diffusion from a cell or grain interior to the cell boundary. The diffusing species is manganese for Al_6Mn and $Al_{12}Mn_3Si$, and silicon for Mg_2Si. For a quadratic concentration profile across a spherical cell, with equilibrium concentration at the boundaries, the growth rate of Al_6Mn constituent can be written as:

$$\left.\frac{df_2}{dt}\right)_g = k_{Mn} \cdot \frac{15 D_{Mn} \cdot \left([Mn] - [Mn]_{e0.6}\right)}{L^2 \cdot \left(\{Mn\}_6 - [Mn]_{e0.6}\right)} \tag{11}$$

where L is the cell half size, $[Mn]_{e0,6}$ is the concentration of manganese in (flat) equilibrium with Al_6Mn, and $\{Mn\}_6$ is the density adjusted concentration of manganese in Al_6Mn and k_{Mn} is a dimensionless tuning parameter. The expressions for growth of $Al_{12}Mn_3Si$ and Mg_2Si constituents are analogous. Since both Al_6 and Al_{12} type phases cannot take all of the manganese flux implied by Equation 11, the total manganese, across cell diffusion is divided into two parts and the growth of both phases is constrained to maintain an equal manganese to iron ratio.

The remaining term in Equation 10 relates to constituent transformation. Analogous to the constituent growth formulation given above, the rate at which constituent is transformed is obtained by assuming that diffusion of silicon to the cell boundary is rate limiting, and by allowing only positive rates. The splitting of incoming silicon for transformation between iron and manganese variants of Al_{12} is addressed by insisting that the transformation does not affect the manganese to iron ratio in the Al_6 type constituents. Also, the rate at which the Al_6 phase disappears is simply obtained by mass balance on iron and manganese.

2.3 Solvus Information

Solute content is calculated from particle volume fractions by mass balance and provides the coupling between the different particle evolution rates. The solvus concentrations have the following forms:

$$[Mn]_{e0,\alpha} = \frac{K_{Mn,\alpha}}{[Si]^{\gamma}} \cdot e^{\frac{-Q_{Mn,\alpha}}{RT}} \quad (12)$$

$$[Si]_{e0,\alpha} = K_{Si,\alpha} \cdot e^{\frac{-Q_{Si,\alpha}}{RT}} \quad (13)$$

The solvus for Al_6Mn is simply the combination of Equations 12 and 13, while the solvus for silicon in equilibrium with Mg_2Si is analogous to Equation 13.

3. AS-CAST STATE

The initial conditions for the evolution equations represent the as cast state. It is assumed that there are no dispersoids as cast, i.e. f_d and N_v are zero. The five constituent volume fractions are calculated for the as-cast state using a measured value of the as cast conductivity, as well as assumptions about iron in solution, fraction of constituent which is Al_{12} type, Fe/Mn ratios in the Al_6 and Al_{12} type phases, and the amount of Mg_2Si.

4. DATA AND FITTING

The model was fit to measured conductivity, observations of constituents (% Al_{12} phase, Mn/Fe ratio in either Al_6 or Al_{12} phase) and dispersoid size.[8-10] Data was considered for large solidification cell sizes (> 50 μm) appropriate to large ingot center positions. Only slow heating and cooling rate (< 1000 °F/hr) data was included (except for quenches at the end of cycles). No data was included where any deformation occurred prior to measurements. Alloy composition ranges in weight % were $0.10 \le Si \le 0.31$, $0.20 \le Fe \le 0.63$, $0.13 \le Cu \le 0.20$, $0.85 \le Mn \le 1.13$ and $0.00 \le Mg \le 1.26$.

The resulting model has goodness of fit as shown in Figures 1 and 2 for conductivity and constituent makeup, respectively. Most of the data is fit fairly well and there is apparently no residual effect of alloy magnesium (Figure 1). The model is described by reasonable parameters for the most part. The number of nucleation sites term, N_{v0} is on the order of 10^4, which is consistent with estimates[5] for site density corresponding to grain boundary nucleation of annealed materials. The dimensionless term B, for reduction of the barrier to nucleation, is on the order of 10^{-2}, which is somewhat smaller than what has been suggested for heterogeneous nucleation.[11] The value obtained for the interfacial energy σ, is 0.26 J/m^2, which is reasonable.[5,7] The solvus terms are fairly consistent with solvus data given by others.[1,12]

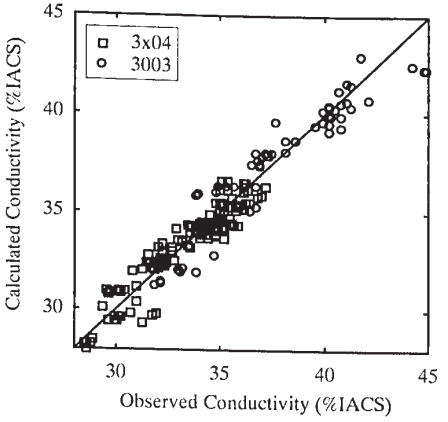

Figure 1. Goodness of fit to conductivity data.

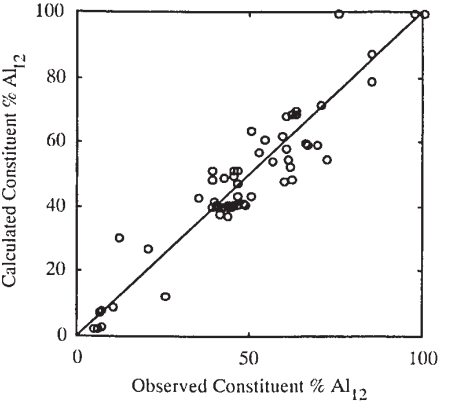

Figure 2. Goodness of fit to constituent percent Al_{12} type phase.

5. APPLICATION OF MODEL

The resulting model can be used to make predictions of dispersoid and constituent precipitation/dissolution kinetics for arbitrary temperature history, prior to any deformation. Example calculations are given in Figure 3 for an alloy containing 0.2 wt% silicon, 0.4 wt% iron, 1.0 wt% manganese, having a cell size of 100 μm and thermally processed as shown. The total volume % of constituent decreases over the course of the transformation, due to the larger density of the Al_{12} phase.

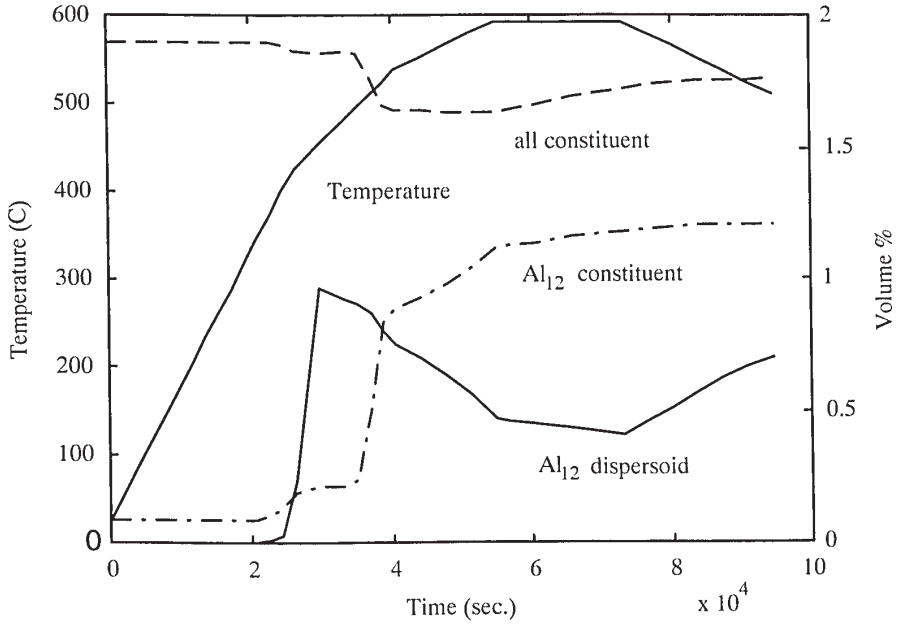

Figure 3. Application of model to simplified preheating cycle.

Further example calculations are given in Figures 4 and 5. In Figure 4 the effect of alloy silicon content on volume % of dispersoid and constituents is shown. This shows the qualitatively necessary result that at some silicon level, here around 0.23 wt%, the constituent as preheated becomes entirely composed of Al_{12} type. This is consistent with experimental results shown by Westerman.[13] The lack of monotonicity in the dispersoid volume% is surprising. The turnaround at low silicon levels may reflect a difficulty in handling low silicon contents, or it may indicate a change of regime, to the formation of Al_6 dispersoids, for example. The turnaround at higher alloy silicon levels seems to correspond to the point at which the constituent becomes entirely Al_{12} type. Thus, it appears that incremental silicon above this point is available to make Al_{12} type dispersoids and thus the volume % dispersoid increases.

In Figure 5 is plotted the effect of alloy iron, analogous to what is shown in Figure 4. Here, there is not surprisingly more constituent as alloy iron increases. Also, increases in alloy iron make for decreases in dispersoid volume %, such that the total amount of Al_{12} type phase, in constituent and dispersoid is roughly constant. This is qualitatively reasonable, since the amount of alloy silicon is fixed in this case. The calculations shown in Figures 4 and 5 are for a specific temperature history, and different results would be obtained for different thermal practice.

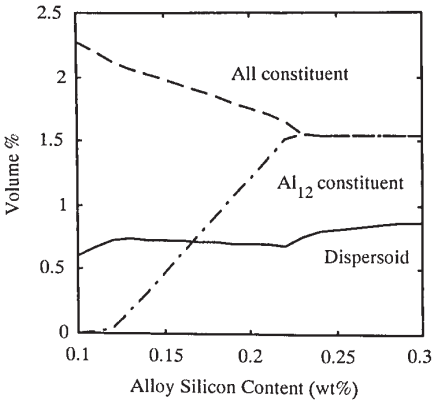

Figure 4. Application of model to the effect of alloy silicon content for 1.0 wt% manganese, 0.4 wt% iron and heating as shown in Figure 3.

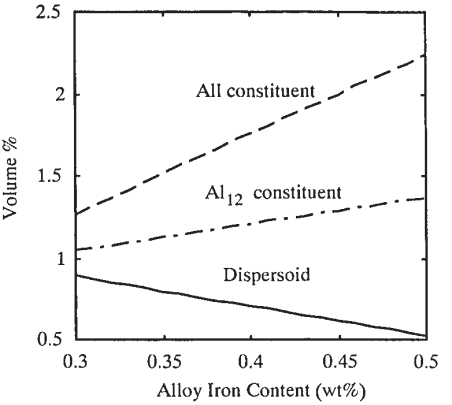

Figure 5. Application of model to the effect of alloy iron content, for 0.2 wt% silicon, 1.0 wt% manganese and heating as shown in Figure 3.

6. SUMMARY

A model was developed for the evolution of dispersoid volume fraction and number density, as well as constituent volume fraction and makeup. The model was satisfactorily fit to large solidification cell size data with alloy manganese in the range of 0.85-1.2 wt%, silicon in the range of .1-.3 wt% and iron in the range of .2-.6 wt%. Example calculations were given, showing the effect of time during the preheating cycle, and the effect of alloy composition on dispersoid and constituent amounts. Future work will attempt to widen the applicability of the model framework to small solidification cell size and more extreme compositions.

REFERENCES

1. H.S. Goodrich, Aluminum Alloys for Packaging, J.G. Morris, et al., Eds., TMS, 1993, pg. 47.
2. Y. Langsrud, et al., Proc. of the 3rd International Conference on Aluminum Alloys, Vol. I, L. Arnbeg, et al., Eds., 1992, pg. 15.
3. A.L. Dons, private communication.
4. J.P. Suni, R.T. Shuey and R.D. Doherty, Aluminum Alloys for Packaging II, J.G. Morris, et al., Eds., TMS, 1996, pg. 145.
5. D.A. Porter and K.E. Easterling, Phase Transformations in Metals and Alloys, Van Nostrand Reinhold Co. Ltd., 1981.
6. R.T. Shuey, unpublished Alcoa work, 1996.
7. J.W. Martin and R.D. Doherty, Stability of Microstructure in Metallic Systems, Cambridge Univ. Press, 1976.
8. T.N. Rouns, Aluminum Alloys for Packaging III, S.K. Das, Ed., TMS, 1998, pg. 3.
9. T.N. Rouns, P.N. Anyalebechi and H.C. Stumpf, unpublished Alcoa work, 1974-1996.
10. T.C. Sun, Aluminum Alloys for Packaging, J.G. Morris, et al., Eds., TMS, 1993, pg. 31.
11. R.D. Doherty, private communication.
12. G. Petzow and G. Effenberg, Eds., Ternary Alloys, pg. 121.
13. E.J. Westerman, Aluminum Alloys for Packaging, J.G. Morris, et al., Eds., TMS, 1993, pg. 1.